Proceedings of the 17th International Conference on Automation & Computing, University of Huddersfield, Huddersfield, UK, 10 September 2011

Numerical Simulation of Natural Frequencies in the Design of Micro Air Vehicle Structures

Yanan Yu (*), Carlo Ferri (**), Qingping Yang (**), and Xiangjun Wang (*)
(*)Tianjin University, State Key Laboratory of Precision Measuring Technology and Instruments, Tianjin, 300072, China
(**)Brunel University, School of Engineering and Design, AMEE, Uxbridge UB8 3PH, UK
yanan.yu@brunel.ac.uk, carlo.ferri@brunel.ac.uk

***Abstract*—The mechanical resonance of structures is often blamed for their collapse. In the attempt to prevent such usually catastrophic events, the identification of the natural frequencies has usually become a constituent part of the design activity of mechanical structures. Micro Air Vehicles (MAVs) are small size unmanned aircraft. This study aims to give a place to the numerical finite element method (FEM) simulations of the natural frequency during the design stage of the MAVs. In particular, the effect of selected materials and geometrical parameters on the simulated first natural frequency has been analyzed in this study. Carbon fibre reinforced polymer (CFRP) appeared to confer the MAV a significant higher first natural frequency than the aluminum alloy investigated (AA2024). Also, given any of the material investigated (CFRP, aramidic fibre reinforced polymer, AA2024), it was found that MAVs simultaneously having a large radius and thickness of the outer shell and a small height have first natural frequency far larger than in any other geometrical configuration.**

Keywords- numerical simulation; finite element method (FEM); natural frequencies of structures; micro air vehicle (MAV); exploratory data analysis (EDA)

I. INTRODUCTION

Small-scale, automatic, unmanned air vehicles are often referred to as 'Micro Air Vehicles' (MAVs) [1] [2]. MAVs play a significant role in many fields of modern world like for example military surveillance, environment monitoring and scientific mapping [3]. Due to the small scale and the light weight MAVs are more sensitive to atmospheric disturbances (e.g. gusts) than other categories of aircraft (e.g. airliners). Assuring flight stability is therefore a prime concern in the design of MAVs [4]. For example, in [5] the stability characteristics and the control properties of hovering MAVs in wind gusts are described.

Beside flight stability, the identification of the mechanical resonant frequencies should also have a part in the process of designing a MAV. The natural frequencies and mode shapes of the dragonfly wing model were investigated by finite element method [6]. The declared intent of such a dragonfly study was to provide some help to the designers of aircraft of similar size. Like for any mechanical or civil structure (shafts, bridges, and buildings), the likelihood that a mechanical natural frequency of the structure becomes equal to that of the applied oscillating loads should be limited. Usually the resonance frequency of an aircraft depends on the scale of the object, its mass, aerodynamic shape, mechanical structure and material [6]. The determination of the natural frequencies of circular cylindrical shells can play a part in the identification of natural frequencies of hovering MAVs. References [7] investigated a shallow spherical shell with large amplitude free vibrations. Reference [8] introduced a novel wave approach to study the vibration characteristics and predict the natural frequencies of circular cylindrical shells.

The prime aim of this study is to estimate the effects of selected design parameters (geometry and material) on the first natural frequency of an aero-elastic ducted-fan hovering MAV. Vertical take-off and landing and hover capabilities are among the main flight characteristics of hovering MAVs [9]. In Fig. 1, an example of a hovering MAV reported in [10] is displayed. The design parameters that significantly affect the natural frequencies of an aircraft structure should be identified during the design process. Knowing which design parameter has an effect on the natural frequencies would in fact enable the designer to make informed decisions to meet the natural frequencies functional requirements requested to the structure. A full factorial design of the numerical experiment is conducted in this study to estimate the effects of selected design parameters on the first natural frequency above mentioned. In Section II, the geometrical proprieties of the hovering MAV design considered in this study are presented. In Section III, the selected materials for the hovering MAV are introduced. In Section IV, the numerical results of the full factorial design for the numerical experiments are presented and discussed. The presentation and discussion method hinge on graphical

Figure 1. Example of a hovering MAV (from [10]).

representations typically used in exploratory data analysis (EDA). The conclusions are then drawn in Section V.

II. Geometry of the Considered Hovering MAV

The aerodynamic shape of the aircraft contributes to determine the aircraft speed, the flight range and the flight stability. Hovering MAVs are typically made up of a shallow spherical shell and a vertical cylindrical duct. The geometry of the hovering MAV design examined in this study is shown in Fig. 2. Four dimensional parameters have been selected to investigate the effect that their values may have on the first natural frequency of the whole structure. For each of the four parameters two values were considered that span the range of values attributable to them without drastically change the overall form of the aircraft. Parameters and values are displayed in Table I.

III. Selection of the Materials

The choice of an aircraft material significantly affects its flight performance. Usually, material and geometry are jointly selected to meet the aerodynamic requirements of the aircraft. In this study, an aluminum alloy and two different composite materials are considered for the hovering MAV design.

Aluminum alloys are typically used in aircraft structures and aerospace applications. Among these, aluminum alloy 2024 is one of the most used materials in aircraft structural components owing to its high strength-to-weight ratio. In particular, such an alloy is traditionally used for wings and fuselages [11].

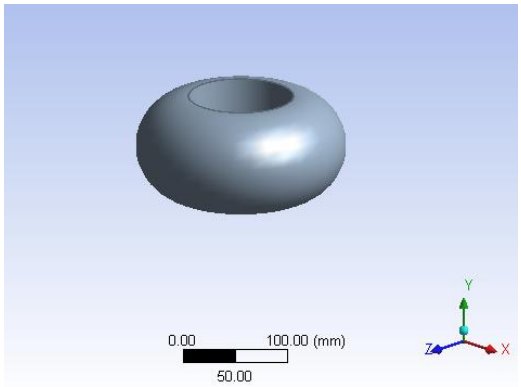

(2a) Hovering MAV geometry.

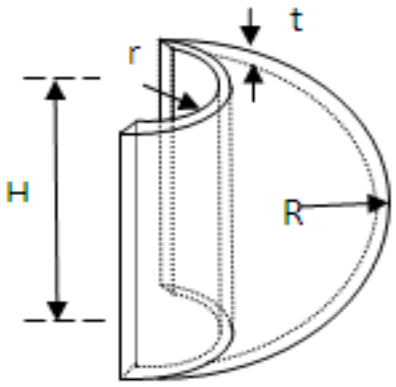

(2b) Geometrical parameters of interest.

Figure 2. The geometry of the hovering MAV. In (2a) the geometry of the whole aircraft is displayed, whereas in (2b) the investigated geometrical parameters are visible.

TABLE I. Geometrical Parameters

Symbol	*Description*	*Low / mm*	*High / mm*
H	Height of the MAV	95	120
R	External radius of the shell	60	100
r	Internal radius of the cylindrical vertical duct	30	60
t	Thickness of the shell	5	10

Composite materials have been given large attention in the latest decades within the aerospace industry because of their high strength and their light weight. From a practical point of view, a composite material can be thought of as a multiphase mixture of at least two solids that are commonly referred to as the matrix and the reinforcement of the composite. In this study, two different composites are considered: an epoxy matrix reinforced with carbon fibre (i.e. carbon-fibre-reinforced polymer, alias CFRP) and an epoxy matrix reinforced with aramidic fibre (i.e. Aramidic-fibre reinforced polymer, alias AFRP). Aramidic fibre is commercially often known as kevlar®. Both CFRP and AFRP contain 60% in volume of the respective fibre. The mechanical properties of these materials are summarized in Table II.

The last column (i.e. E/ρ) has been calculated from the second and the fourth to represent the rigidity per unit of mass of one centimetre cubic of material. This ratio highlights that CFRP has a much higher strength-to-weight ratio than the other two materials considered.

IV. Results and Discussion

The numerical simulations performed in this study have been conducted using the algorithms implemented in a commercially available piece of software for modal frequency analysis with finite element method (FEM). A detailed theoretical background for such algorithms can be found for instance in chapter one, two, four and twelve of [13]. In the formulation of the numerical problem, the displacement field has been constrained to be zero on the inner cylindrical surface of the hovering MAV vertical duct. Such a constraint constitutes the boundary condition of the problem.

TABLE II. Mechanical Properties of Materials

Materials	**Mechanical properties**			
	Young's modulus, E/GPa	***Poisson Ratio, ν***	***Density, ρ/ g·cm^{-3}***	***E·ρ^{-1}/ GPa·cm^{3}·g^{-1}***
Aluminum 2024[a]	72.4	0.33	2.77	26.14
CFRP[a]	220	0.25	1.70	129.41
AFRP[a]	76	0.34	1.4	54.29

a. Data from [12].

The four geometrical factors examined (H, R, r, t) have two levels each, whereas the factor material has three levels. The full factorial design of the numerical experiments therefore encompasses 48 different experimental cases (i.e. 3*2^4). The first natural frequency numerically estimated as described above has been selected as the response variable. Running a full factorial design has enabled the authors to provide a graphical estimation of both the effects of the factors on the numerically estimated first natural frequency and the second order interaction effects between the factors.

A. Main effects

For the main effects, notched box plots have been used to display the results and to estimate graphically if some significant difference between them is present. In a box plots with notches three lines are represented: the 25% percentile, the median and the 75% percentile. The vertical v-groove on the box with apex on the median line is calculated in such a way that if the v-grooves of two boxes are vertically overlapping, and then there is little evidence that the median of the two boxes are significantly different. Also, the distance between the 25% and 75% percentiles allows the investigator to draw conclusions about the dispersion of the response variable for that specific level of the factor under examination. Values of the frequency that lie outside the vertical segments stemming from the box (aka whiskers) should in general deserve further examination in most of the cases. This is to identify possible anomalies occurred in the experimental procedure. More details about box plots and box plots with notches can be found in [14] and [15], respectively. All the figures in this section have been produced using the GPL'd software R, available free of charge at the R-project website (i.e. www.r-project.org). In this qualitative approach, the median has been implicitly used to estimate the centrality parameter of the distribution of values of the simulated frequency for each level of the factor under investigation. In most cases a mean is instead used. However, using the median as estimator of centrality constitutes an approach more robust to the presence of extreme values in the data. As it is shown in the analysis here below, that is the case with the data available in this investigation.

From Fig. 3, the effect of the material on the first natural frequency can be qualitatively estimated. The dispersion of the first natural frequency for each of the materials investigated appears comparable (i.e. comparable vertical heights of the boxes). The CFRP seems to provide a significant higher first natural frequency than Aluminum 2024 (the vertical v-groves of the correspondent boxes do not overlap). However, a significant difference between Aluminum and AFRP does not appear. Also, it is quite difficult to ascertain whether the difference between AFRP and CFRP is significant: the v-grooves of the correspondent boxes are border-line overlapping. In Fig. 3, six extreme values that depart from the majority of the data for a given material are observed (they are represented as points in Fig.4). A closer scrutiny of these six values reveals that they are obtained in identical combinations of the levels of three factors different from material. Namely, they are obtained

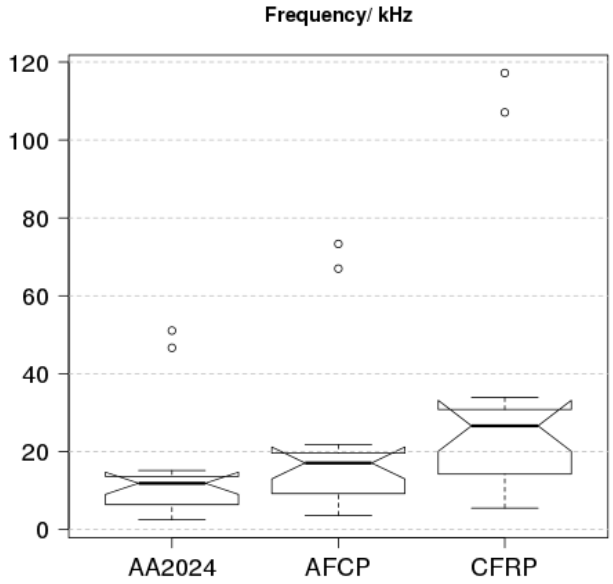

Figure 3. Box plots of the frequency grouped by material.

for a large external radius (R=100 mm), a great thickness of the shell (t=10 mm), a short height of the MAV (H=95 mm). Also it is noticed that for such combination of levels, increasing the internal radius r from 30 to 60 mm always results in an increment of the simulated first natural frequency for any of the materials considered.

The effect of the external radius on the response variable can be qualitative estimated from Fig. 4. The simulated frequency displays a distribution of values that is more dispersed when using a 100mm external radius than when using 60mm external radius. It then seems more useful to choose a larger external radius, if the design intent is to increase the first natural frequency of the aircraft structure. Also, in Fig. 4, when R=100 mm, two values appears as extreme. A further examination reveals that such a pair of values is among the six out-lying points already discussed in Fig.3.

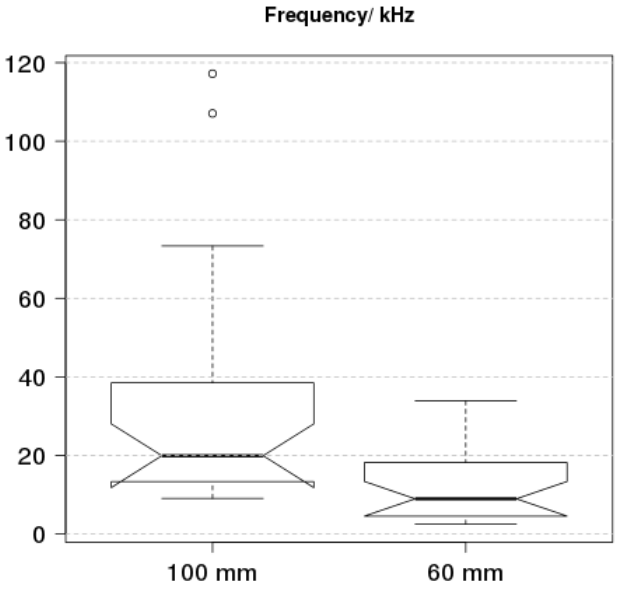

Figure 4. Box plots of the frequency grouped by external radius (R).

As displayed in Fig. 5, a very similar situation happens when considering the effect of the height factor on the simulated first frequency. Lower heights of the hovering MAV (i.e. lower H) are likely to increase significantly the first natural frequency of the aircraft.

A close examination of the box plots for the internal radius and the thickness did not reveal any significant effect of these two factors on the simulated first natural frequency. For this reason they have not been included in this section. The sole noteworthy comment about them is that the variability of the simulated frequency appears larger at 10 mm thickness than it is at 5 mm.

B. Second order interaction effects

The effect that a factor, say factor A, have on the simulated first natural frequency may be different when different levels of the other factors involved in the analysis are considered. An interaction plot shows the mean (alias average) of the response for the levels of the factor investigated appearing on the abscissa when the levels of a second factor is also used to subset the data. Joining the means at the same level of the second factor is therefore a means to estimate qualitatively if the two factors in the plot may interact when affecting the response variable. In particular, if the lines so obtained are crossing or tend to cross, then it can be argued that there may be a different effect of the factor on the abscissa on the response variable at different levels of the other factor displayed in the interaction plot. Shortly, there is a strong suspicion of an interaction between the two factors.

As shown in Fig. 6, when t=10 mm, changing the external radius from 60 mm to 100 mm will give a large frequency increment (in the order of 35 kHz). But when t=5 mm, the frequency will have a relatively small increment (in the order of 7 kHz). From a designer perspective, The implications of this finding is that changing the external radius of the outer shell may have quite an unpredictable outcome on the frequency depending on the thickness of the shell itself.

Similar situation appears also for the interaction

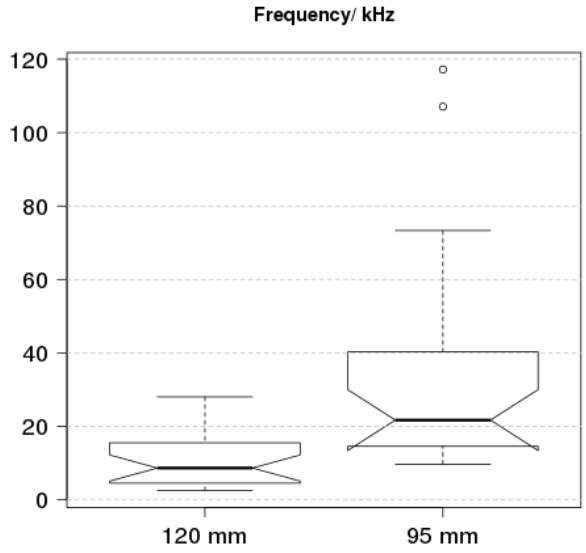

Figure 5. Box plots of the frequency grouped by height (H).

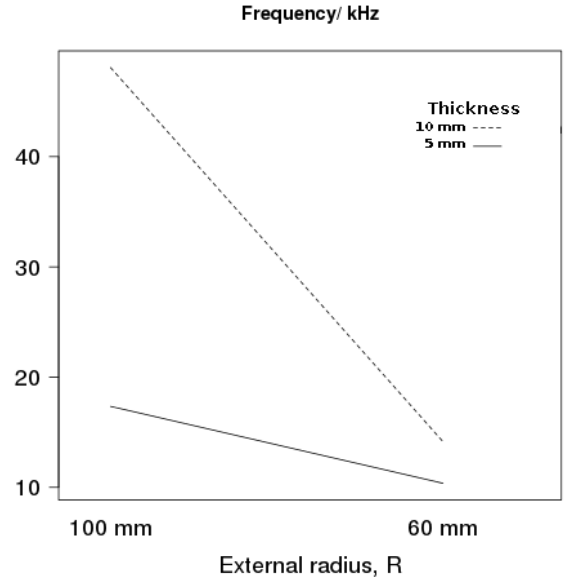

Figure 6. Interaction plot of the external radius (R) and the thickness (t).

between height and thickness. In Fig. 7, with t=10 mm, when decreasing the height of the MAV from 120 mm to 95 mm, there is a suspicion that the natural frequency increases significantly more than with t=5 mm. From a practical perspective, this finding may for example be useful to a designer that is constrained to use an outer shell with t= 10 mm. He/she would know that he/she would probability have better chances of increasing the first natural frequency of the MAV by reducing the height of the structure. But not so, if he/she had been given the constraint t=5 mm.

Fig. 8 can give a qualitative idea of the interaction effect of the internal radius and the thickness. In Fig.8, when t=10mm, changing the internal radius from 30 mm to 60 mm leads to an increment of the first natural frequency. But when t=5 mm, the same change of the internal radius causes the first natural frequency to drop. A mild interaction may therefore be present between these

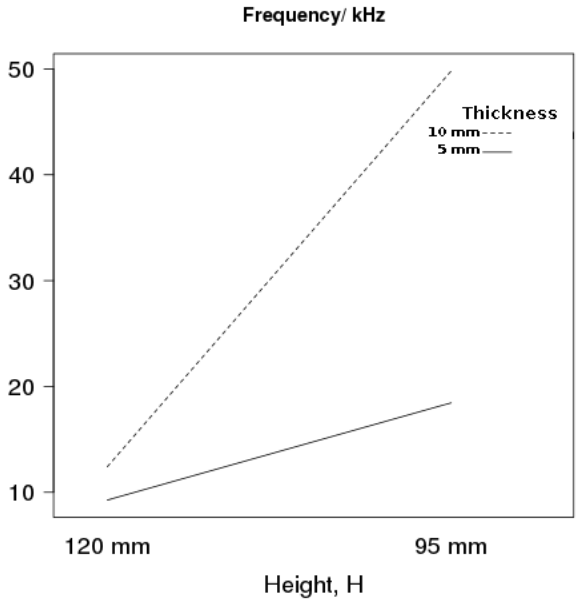

Figure 7. Interaction plot of the height (H) and the thickness (t).

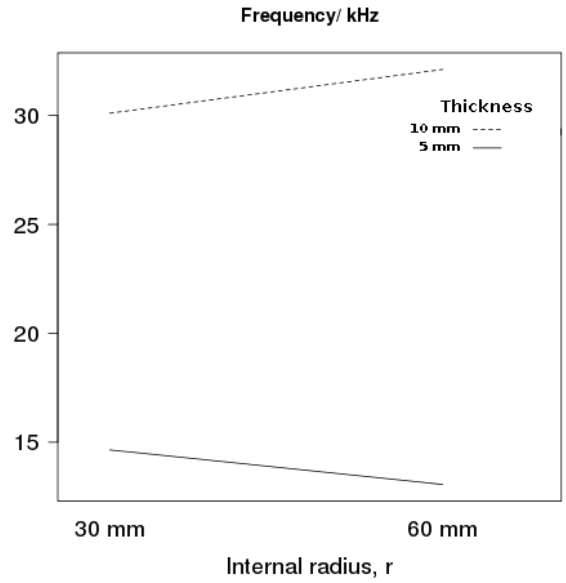

Figure 8. Interaction plot of the internal radius (r) and the thickness (t).

two factors. All the remaining 10-3=7 second order interaction plots have been analyzed like here above. Yet no interesting additional comments could be elicited from them. For these reason they have been omitted from this section.

V. CONCLUSIONS

The identification of the natural frequencies of a mechanical structure is an integral part of its design phase. In particular, this should hold also for aerospace applications such as the design of a hovering micro air vehicle. The effect of selected materials and geometrical parameters on the simulated first natural frequency has been analyzed in this study. The numerically simulated values of the first natural frequency were obtained using the modal frequency analysis algorithms implemented into commercially available FEM software. Aluminum alloy 2024, carbon fibre reinforced polymer and aramidic fibre reinforced polymer were selected as materials, whereas four geometry parameters have been changed at two different levels. This setting resulted in 48 cases of a full factorial numerical experiment. The results were analyzed using graphical representations typical of exploratory data analysis (EDA). The main findings of this investigation are:

- Carbon fibre reinforced polymer appeared to provide first natural frequencies higher than the aluminum alloy. Yet no significant difference appeared between the first natural frequency of aluminum alloy and aramidic fibre reinforced polymer. It is unclear however if carbon fibre provides higher first natural frequencies than aramidic fibre when used in the investigated composites.
- If a material has been selected, then the geometry that appears to give a considerable higher first natural frequency is characterized by large radius of the outer shell, great thickness of such a shell and small height of the MAV.
- Both the radius of the cylindrical duct and the thickness of the shell do not appear to have significant effect on the first natural frequency. Instead, increasing the radius of the outer shell seems to significantly yield higher first natural frequencies. Likewise does reducing the height of the MAV.
- Second order interactions between the investigated factors have been discussed. But not clear interaction effect is apparent.

REFERENCES

[1] T.T.H. Ng and G.S.B. Leng, "Application of genetic algorithms to conceptual design of a micro-air vehicle," Engineering Applications of Artificial Intelligence, vol. 15, pp. 439-445, September 2002.

[2] Bor-Jang Tsai and Yu-Chun Fu, "Design and aerodynamic analysis of a flapping-wing micro aerial vehicle," Aerospace Science and Technology, vol. 13, pp. 383-392, October-November 2009.

[3] Takeo Kanade, Omead Amidi, and Qifa Ke, "Real-time and 3D vision for autonomous small and micro air vehicles," 43rd IEEE Conference on Decision and Control Bahamas, vol. 2, pp. 1655-1662, December 2004.

[4] Richard J. Bachmann, Frank J. Boria, Ravi Vaidyanathan, Peter G. Ifju, and Roger D. Quinn, "A biologically inspired micro-vehicle capable of aerial and terrestrial locomotion," Mechanism and Machine Theory, vol. 44, pp. 513-526, March 2009.

[5] Jean Michel Pflimlin, Philippe Soueres, and Tarek Hamel, "Hovering flight stabilization in wind gusts for ducted fan UAV," 43rd IEEE Conference on Decision and Control Bahamas, vol. 4, pp. 3491-3496, December 2004.

[6] H. Rajabi, M. Moghadami, and A. Darvizeh, "Investigation of microstructure, natural frequencies and vibration modes of dragonfly wing," Journal of Bionic Engineering, vol. 8, pp. 165-173, June 2011.

[7] D.N. Paliwal, H. Kanagasabapathy, and K.M. Gupta, "Vibrations of an orthotropic shallow spherical shell on a Kerr foundation," International Journal of Pressure Vessels and Piping, vol. 64, pp. 17-24, 1995.

[8] C. Wang and J.C.S. Lai, "Prediction of natural frequencies of finite length circular cylindrical shells," Applied Acoustics, vol. 59, pp. 385-400, April 2000.

[9] Eric N. Johnson and Michael A. Turbe, "Modeling, control, and fight testing of a small ducted fan aircraft," AIAA Guidance, Navigation, and Control Conference and Exhibit California, pp. 1-23, August 2005.

[10] http://www.aviationweek.com/aw/.

[11] http://www.aviationmetals.net/2024_aluminum.php.

[12] William D. Callister, Jr, Materials Science and Engineering: An Introduction, 6th ed., New York; Chichester: Wiley, 2003, pp. 737-745.

[13] Robert D. Cook, Concepts and Applications of Finite Element Analysis: A Treatment of the Finite Element Method as used for the Analysis of Displacement, Strain, and Stress, New York; London (etc.): Wiley, 1974.

[14] John W. Tukey, Exploratory data analysis, Addison-Wesley, 1977, section 2c.

[15] Robert McGill, John W. Tukey, and Wayne A. Larsen, "Variations of box plots," The American Statistician, vol. 32, pp. 12-16, February 1978.